David S. McLachlan
and Godfrey Sauti

The AC And DC Conductivity (Dielectric Constant) Of Composites

This paper will show how to analyze the AC and DC conductivity, or complex dielectric constant, of binary (a conducting and an insulating phase)-composites (media, compacts), where the better conducting component has a volume fraction ϕ. Most binary and some tertiary media (with some ingenuity the analysis can be applied to tertiary media), are found in practice to at least approximate one of the two basic micro(nano)structures [1]. The first are matrix dominated media, where the matrix phase surrounds the granular (particle) phase at all volume fractions. These are usually best described using the Maxwell Wagner Effective Media Equation (also known as the Maxwell-Garnet equation). The Maxwell-Wagner model is formally equivalent to the Hashin-Shtrikman [2] lower bound (insulator host) and upper bound (conductor host) [3, 4]. For matrix dominated media, the Bricklayer Model [5] is also useful. Matrix dominated media are not dealt with in detail this in paper. The second micro (nano)-structure is where the conducting particles, in a two phase material, can make electrical contact with each other, when their volume fraction ϕ reaches a certain critical ϕ_c, where a continuous conducting path or spanning cluster forms [1]. The complex electrical conductivity of these systems is best [6, 7] described by the Two Exponent Phenomenological Percolation Equation (TEPPE)(also known as the General Effective Medium (GEM) equation) [8–18]. The three standard percolation equations are reviewed in [19–21], but it is shown in [6] and [7] that, while the single TEPPE reduces to the three standard equations in the appropriate limits, it is far superior

in the second order terms (i.e. the imaginary dielectric constant ε_{mi} in the conducting media above ϕ_c and the dielectric loss ε_{ii} (or σ_{mr}) below). The theory given here applies to nano, micro and macro media.

The AC conductivity of the media (composite) (σ_m) is the sum of the real and imaginary conductivities, which is given by $\sigma_m = \sigma_{mr} + i\sigma_{mi}$. The conductivity of the more conducting component is given by $\sigma_c = \sigma_{cr} + i\sigma_{ci}$ or simply $\sigma_c = \sigma_{cr}$ if ideal conductivity ($\sigma_{cr} \gg \sigma_{ci}$) is assumed. For the insulating component, the conductivity is $\sigma_i = \sigma_{ir} + i\sigma_{ii}$ where $\sigma_{ii} = \omega\varepsilon_0\varepsilon_{ir}$. σ_i is often approximated as $\sigma_i = i\omega\varepsilon_0\varepsilon_{ir}$ (i.e $\sigma_{ir} \ll i\sigma_{ii}$). In practice, σ_{ir} incorporates both a, usually very small, DC conductivity and the dielectric polarization loss term ($\omega\varepsilon_0\varepsilon_{ii}$). The expressions for σ_c and σ_i can be frequency and/or temperature dependent. The complex conductivity and dielectric constant are related by $\sigma = \omega\varepsilon_0\varepsilon$. As the critical volume fraction ϕ_c is of great importance, its origins are briefly described here. A more detailed account can be found in [1, 3, 22]. If conducting spheres, of just sufficient size to touch their nearest neighbors, are placed at random on the sites of 3d Bravais lattices it is found that ϕ_c is 0.16 ± 0.02 [3, 23]. If equally sized conducting and insulating spheres are placed at random in a container, ϕ_c is also found to be about 0.16. This value of ϕ_c is often taken to characterize 3d random media but other values of ϕ_c are permitted [3, 22]. For $\phi_c < 0.16$ three models can be considered (for $\phi_c > 0.16$ see [24]). The first is the grain consolidation model [3, 22] where randomly nucleated insulating spheres have grown (been sintered) so as to confine the conducting material to inter granular channels. At a ϕ value of 0.03 (ϕ_c) the channels become isolated. The second model comprises of granular structures [14] where a fine conducting powder coats a coarse insulating one. Calculations for ϕ_c, based on there being a percolation path on the surface of the insulating spheres, have been made

by Kusy [25]. For instance, when the ratio of the radii of the components is 30, $\phi_c \approx 0.03$. For particles with irregular geometries, especially extended ones (rods, discs) one must use the excluded volume model of Balberg *et al.* [26]. For rods with a length to width ratio of 10, $\phi_c \approx 0.1$, while for a ratio of 1000, $\phi_c \approx 0.001$.

Note that no experimental details will be given here, for these the reader should consult the original papers. As previously stated a recent series of papers [8–12, 14–16] has shown that the TEPPE which is:

$$(1-\phi)\frac{\sigma_i^{1/s} - \sigma_m^{1/s}}{\sigma_i^{1/s} + A\sigma_m^{1/s}} \qquad (1)$$
$$+\phi\frac{\sigma_c^{1/t} - \sigma_m^{1/t}}{\sigma_c^{1/t} + A\sigma_m^{1/t}} = 0,$$

with $A = (1 - \phi_c)/\phi_c$ and the exponents s and t, best describes experimental results for percolation systems, especially the second order terms [11, 12].

Equation (1) yields the two limits for $|\sigma_c| \to \infty$:

$$\sigma_m = \sigma_i\left(\frac{\phi_c}{\phi_c - \phi}\right)^s \text{ or}$$
$$\varepsilon_{mr} = \varepsilon_{ir}\left(\frac{\phi_c}{\phi_c - \phi}\right)^s,$$
$$\phi < \phi_c, \qquad (2)$$

and $|\sigma_i| \to 0$:

$$\sigma_m = \sigma_c\left(\frac{\phi - \phi_c}{1 - \phi_c}\right)^t \text{ or}$$
$$\varepsilon_{mr} = \varepsilon_{ir}\left(\frac{\phi - \phi_c}{1 - \phi_c}\right)^t,$$
$$\phi > \phi_c. \qquad (3)$$

These equations are the normalized standard percolation results [19, 20] and characterize the exponents s and t. In the crossover region, where $\phi \cong \phi_c$ and

$$\phi_c - (\sigma_i/\sigma_c)^{1/t+s} < \phi <$$
$$\phi_c + (\sigma_i/\sigma_c)^{1/t+s} \qquad (4)$$

or

$$\phi_c - (\omega\varepsilon_0\varepsilon_{ir}/\sigma_{cr})^{1/t+s} < \phi <$$
$$\phi_c + (\omega\varepsilon_0\varepsilon_{ir}/\sigma_{cr})^{1/t+s} \qquad (5)$$

holds, Eq. (1) gives

$$\sigma_m \approx \sigma_i^{t/(s+t)} \sigma_c^{s/(s+t)} \qquad (6)$$

or

$$\sigma_m \approx (\omega\varepsilon_0\varepsilon_{ir})^{t/(s+t)} \sigma_{cr}^{s/(s+t)}, \quad (7)$$

which is in agreement with the theory given in [19] and [20].

Eq. (6) shows that, in the crossover region, the conductivity σ_{mr} should be proportional to $\omega^{t/(s+t)}$ and the dielectric constant ε_{mr} (recall that $\varepsilon_{xy} = \sigma_{xy}/\omega\varepsilon_0$), is proportional to $\omega^{s/(s+t)}$. Note that Eqs. (2) and (3) are not valid in the crossover region.

Arguably the best DC conductivity results, for a percolation system, are those measured on compressed Graphite-hBN discs, which are given in Fig. 1, from which ϕ_c, s, t, σ_c and σ_i can easily be determined using Eq. (1) [8].

Figure 2 shows the AC conductivity plotted as a function of frequency for a loosely packed Graphite-hBN mixture [9]. Note how one can clearly distinguish between samples above and below ϕ_c.

It should be noted that the conductivities, below ϕ_c in Fig. 2, contain contributions due to the isolated conducting clusters and the dielectric loss of the insulating component. In most other systems such conductivity results are dominated by the contributions of the insulating component.

A system where the conducting clusters clearly dominate is given in [11]. Figure 3 [11] shows that the dielectric constants as a function of frequency are not even qualitatively in accord with the predictions of the standard equations, (Eqs. (2) & (3) and [19–21]).

Note that the top most curve is for a sample above ϕ_c. Further, a close examination of Fig. 3 shows that if the results are re-plotted as $\log(\varepsilon_{ir})$ as a function of $\log|\phi-\phi_c|$, the values obtained for s will be frequency dependent, a fact first pointed out in [14]. Second order dielectric results of this nature can be qualitatively fitted using Eq. (1) [11], but a more complex model is needed to fit these results more accurately [12]. AC conductivity results can be fitted using Eq. (1) as demonstrated in [17,18]. However it is more usual to scale all the results onto a single master curve first. This is done by dividing each AC conductivity curve (plotted as a function of
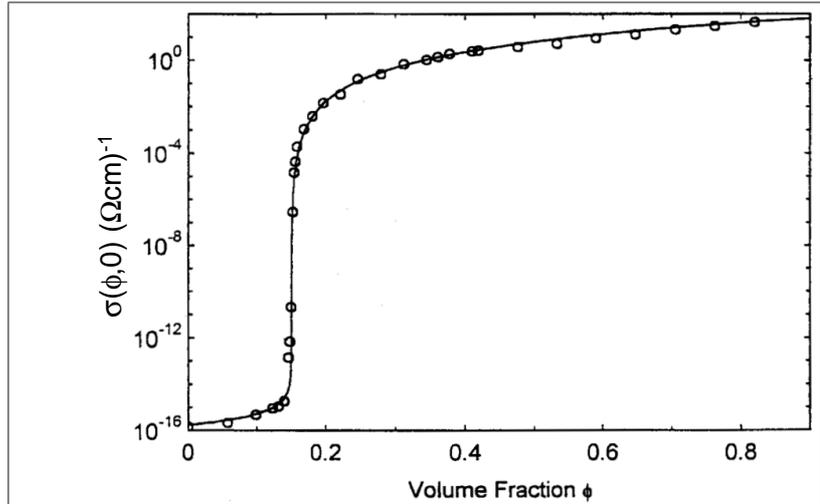
Fig. 1: DC percolation results for Graphite-hBN discs. The continuous line is obtained from Eq. (1) using $\phi_c = 0.150 \pm 0.002$,
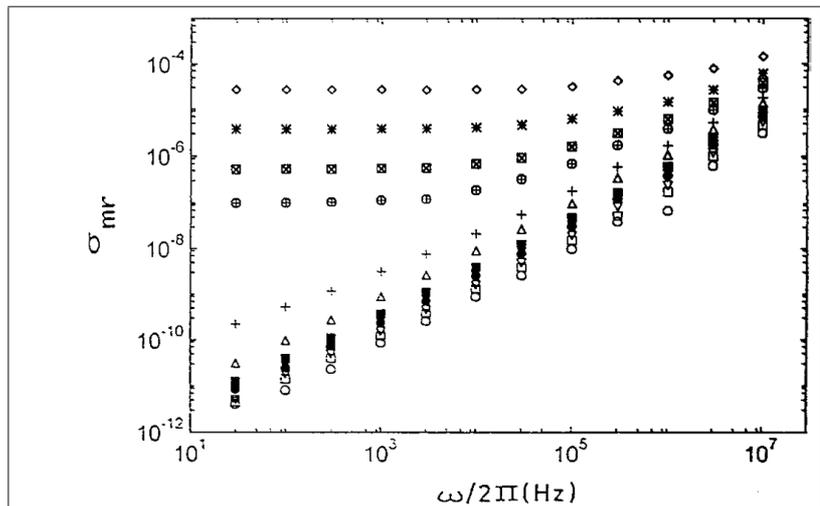
Fig. 2: AC conductivity plotted against frequency for a loosely packed Graphite-hBN mixture. The range of ϕ values is between 0.112 and 0.133. A gap occurs between the low frequency results above and below ϕ_c.
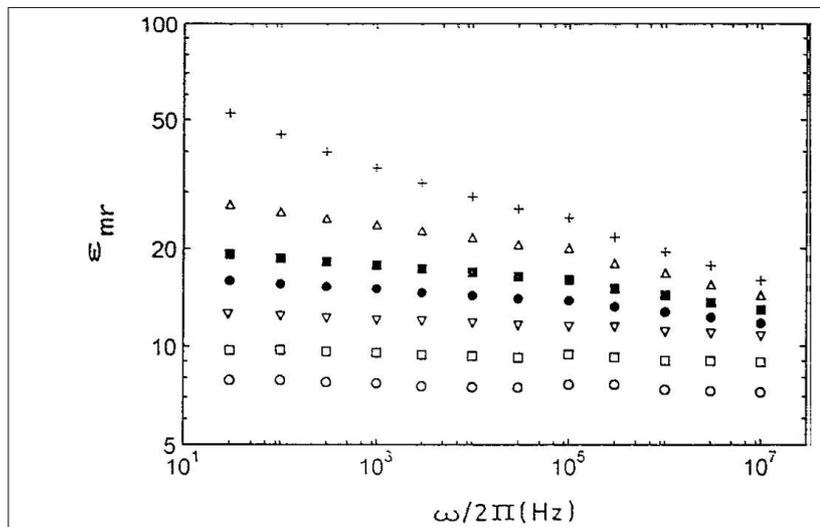
Fig. 3: Dielectric constant plotted against frequency for a loosely packed Graphite-hBN mixture. The range of ϕ values is between 0.112 and 0.123. The top curve is for a sample marginally above ϕ_c.

frequency) by the DC conductivity and then sliding the $\log(\sigma_{cr}(\phi,\omega)/\sigma_{cr}(\phi,0))$ results along the $\log(1)$ axis, by a factor $(1/\omega_c)$, till the results coincide (see fig. 4).

The scaling functions $F_-(\omega/\omega_c)$ and $F_+(\omega/\omega_c)$ are given by,

$$\sigma_m = \sigma_c \left(\frac{\phi_c - \phi}{\phi_c} \right)^t F_- \left(\frac{\omega}{\omega_c} \right), \quad (8)$$

for $\phi < \phi_c$ and

$$\sigma_m = \sigma_c \left(\frac{\phi - \phi_c}{1 - \phi_c} \right)^t F_+ \left(\frac{\omega}{\omega_c} \right) \quad (9)$$

for $\phi > /\phi_c$. Here, σ_m may originate either from theoretical calculations, using Eq. (1), or experimental results.

This is shown in Fig. 4 and shows that Eq. (1) can be used to fit AC conductivity results from experiment. In this case the DC values of the parameters ϕ_c, s, t, σ_c and σ_i, were used in deriving $F_-(\omega/\omega_c)$ and $F_+(\omega/\omega_c)$, but in most cases different values of s and t have to be used to obtain a satisfactory fit.

Note that Eq. (1), with complex conductivities, is not easy to solve. However, a Mathematica package which does this is available from godfrey_sauti@yahoo.com. A further publication in an upcoming newsletter will deal with scaling and universality in more depth and explain why the ω_c values obtained from experiment and theory do not agree, as well as, show how ω_c can be calculated directly from impedance curves where these are available [15, 16].

Unfortunately the values of s and t do not tell one much about the microstructure of the media but does indicate some thing about the inter-particle (inter-cluster) resistances. The universal value of exponent t (t_{un}), which is usually observed in computer simulations and for "ideal" systems, is 2.0. It was shown theoretically and by computer simulations [27] that if the low conductance bonds in the percolation network, or the inter-granular conductances of the conducting component in a continuum system, have a very wide distribution, then t can be larger than t_{un}. This distribution can be due to a large range of effective geometrical resistivity factors in a continuous homogeneous conduct-
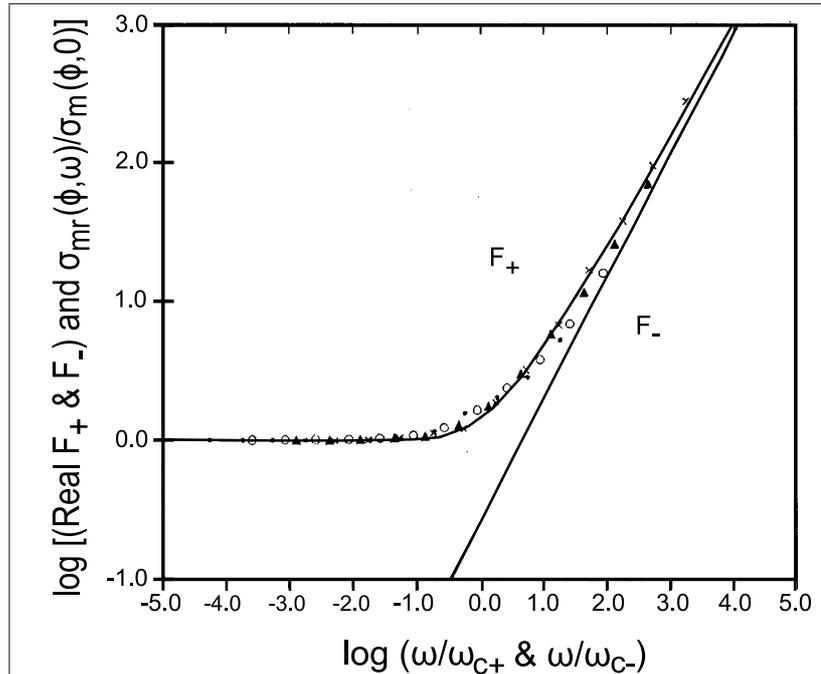
Fig. 4: A plot of the log of the scaled conductivities against the log of the scaled frequency for a 55%G - 45%BN powder. The origin of the F_+ and F_- plots onto which the experimental curves are scaled along the (ω/ω_{c+}) or (ω/ω_{c-}) axis is discussed in the text and in greater detail in [9].

ing phase, of a medium such as a Swiss Cheese (which contains Random Voids) [28, 29]. In this model a range of very thin and highly resistive threads of conductor (cheese), between the large overlapping voids (air), give rise to a wide distribution in the conductances between the more extended or bulky regions of conductor. This model give values for t in the range 2.0-2.5, but an extension of it allows far higher values [30]. A model which considers the conducting paths in terms of Links, (large conducting) Blobs and Nodes (multiple link sites) gives an upper limit of 2.35. Note that all of the above models assume a homogeneous (non-granular) conducting phase. A model for granular conducting systems [31,32], based on the dominant resistances in the current carrying Links and Blobs (now consisting of a granular conductor), being due to a large range of inter particle tunneling contacts has been proposed. In virtually all media with a granular conducting phase $t > t_{un}$ is observed due to a range of inter particle tunneling distances [33]. A combination of the Swiss Cheese and tunneling model which would further enhance t has also been proposed [34].

This paper has shown how the AC

and DC conductivity (dielectric constant) results can be analyzed in terms of the Two Exponent Phenomenological Percolation (TEPPE) equation. As the actual complex conductivities appear in the expressions it is theoretically possible to determine the dispersive conductivities for both components and, for percolation systems, the critical volume fraction as well as the exponents s and t. In practice, even when a large amount of data is available on both sides of the critical volume fraction, this is a formidable task. Therefore, it is usually advisable to know, or measure or model, the complex conductivity of at least one of the components first. Note that in a real medium the conductivity, especially that of a granular conductor, may be modified by surface reactions or dominated by inter particle contacts.

References

[1] David S. McLachlan, Godfrey Sauti, Journal of Nanomaterials 2007 (2007).

[2] Z. Hashin, S. Shtrikman, J. Appl. Phys. 33 (1962) 3125.

[3] David S. McLachlan, Michael Blaszkiewicz, Robert E. Newnham, J. Am. Ceram. Soc. 73 (1990) 2187.

[4] M.A. Campo, L.Y. Woo, T.O. Ma-

son, E.J. Garboczi, J. Electroceram. 9 (2002) 49.

[5] Jin-Ha Hwang, D.S. McLachlan, T.O. Mason, J. Electroceram 3 (1999) 7.

[6] D. S. McLachlan, C. Chiteme, W. D. Heiss, Junjie Wu, Physica B 338 (2003) 256.

[7] D. S. McLachlan, C. Chiteme, W. D. Heiss, Junjie Wu, Physica B 338 (2003) 261.

[8] Junjie Wu, D. S. McLachlan, Phys. Rev. B 56 (1997) 1236.

[9] Junjie Wu, D. S. McLachlan, Phys. Rev. B 58 (1998) 14880.

[10] D. S. McLachlan, Michael B. Heaney, Phys. Rev. B 60 (1999) 12746.

[11] D. S. McLachlan, W. D. Heiss, C. Chiteme, Junjie Wu, Phys. Rev. B 58 (1998) 13558.

[12] W. D. Heiss, D. S. McLachlan, C. Chiteme, Phys. Rev. B 62 (2000) 4196.

[13] Christian Brosseau, J. Appl. Phys. 91 (2002) 3197.

[14] C. Chiteme, D. S. McLachlan, Phys. Rev. B 67 (2003).

[15] Cosmas Chiteme, David S. McLachlan, Godfrey Sauti, Phys. Rev. B 75 (2007) 094202.

[16] David S. McLachlan, Godfrey Sauti, Cosmas Chiteme, Phys. Rev. B 76 (2007).

[17] Ian J. Youngs, Ph.D. thesis, Electronic and Electrical Engineering, University College, London, 2001.

[18] Ian J. Youngs, J. Phys. D: Appl. Phys. 35 (2002) 3127.

[19] J. P. Clerc, G. Giraud, J. M. Laugier, J. M. Luck, Adv. Phys. 39 (1990) 191.

[20] D. J. Bergman, D. Stroud, Solid State Phys. 46 (1992) 148.

[21] Ce-Wen Nan, Progress in Materials Science 37 (1993) 1.

[22] David S. McLachlan, J. Electroceram 5 (2000) 93.

[23] Richard. Zallen, The Physics of Amorphous Solids, Wiley-Interscience, New York, 1983.

[24] D. S. McLachlan, R. Rosenbaum, A. Albers, G. Eytan, N. Grammatica, G. Hurvits, J. Pickup, E. Zaken, J. Phys.: Condens. Matter 5 (1993) 4829.

[25] R. P. Kusy, J. Appl. Phys. 48 (1977) 5301.

[26] I. Balberg, C. H. Anderson, S. Alexander, N. Wagner, Phys. Rev. B 30 (1984) 3933.

[27] P. M. Kogut, J. P. Straley, J. Phys. C 12 (1979) 2151.

[28] B. I. Halperin, Shechao Feng, P. N. Sen, Phys. Rev. Lett. 54 (1985) 2391.

[29] Shechao Feng, B. I. Halperin, P. N. Sen, Phys. Rev. B 35 (1987) 197.

[30] I. Balberg, Phys. Rev. B 57 (1998) 13351.

[31] H. E. Stanley, J. Phys. A: Math. Gen. 10 (1977) L211.

[32] A. Coniglio, J. Phys. A: Math. Gen. 15 (1982) 3829.

[33] I. Balberg, Philos. Mag. B 56 (1987) 991.

[34] C. Chiteme, D. S. McLachlan,

I. Balberg, Phys. Rev. B 67 (2003).

[35] N. F. Mott, E. A. Davies, Electronic Processes in Noncrystalline Solids, Clarendon, Oxford, 1979.

David S. McLachlan[1,2,*] and Godfrey Sauti [1,3,†]

[*]davidsm@sun.ac.za
[†]godfrey.sauti@nianet.org
[1]Department of Chemistry and Polymer Science, University of Stellenbosch, P. Bag X1, Matieland 7602, South Africa.
[2]Materials Physics Research Institute and School of Physics, University of the Witwatersrand, P. Bag 3, Wits 2050, South Africa.
[3]National Institute of Aerospace, 100 Exploration Way, Hampton, VA 23666, USA.

Bernhard Roling and Sevi Murugavel

Nonlinear Ionic Conductivity of Solid Electrolytes

For electrochemical energy storage and conversion applications, such as batteries and fuel cells, the use of solid electrolytes offers several advantages over conventional liquid electrolytes based on aqueous or organic solvents. In particular, solid electrolytes exhibit often a higher chemical and electrochemical stability, resulting in reduced safety problems in batteries. Furthermore, miniaturised electrochemical cells, such as microbatteries [1], can be manufactured based on multilayer stacks of thin electrode and electrolyte films. The application of thin electrolyte films offers the additional advantage that the electrical resistance of the film decreases with decreasing thickness. For calculating the electrical resistance, one has to take into account, however, that in a thin film even a small voltage drop may cause a high electric field resulting in a field-dependent (nonlinear) ionic conductivity. For instance, a dc voltage drop of 5 V in an electrolyte film with a thickness between 100 nm and 1 μm leads to a dc electric field between 500 kV/cm and 50 kV/cm. In this field range, the resulting dc current density j depends on the dc field E in a nonlinear fashion:

$$j(E) = \sigma_1 E + \sigma_3 E^3 + \sigma_5 E^5 + \dots \quad (1)$$

In this power series, σ_1 denotes the low-field conductivity, while σ_3, σ_5 etc. are higher-order conductivity coefficients.

The simplest theoretical approach to interpret this nonlinear electrical behaviour is to consider a simple regular hopping model with distance a between adjacent sites. For this model it turns out that [2]

$$j(E) \propto \sinh(q\,a\,E/(2k_BT)). \quad (2)$$

This expression implies that in the framework of this model, it is possible to extract the elementary hopping distance a from field-dependent electrical data.

Therefore, one may use the two lowest coefficients σ_1 and σ_3 of the power series of $j(E)$ to define an apparent jump distance a_{app} via

$$(a_{app})^2 \equiv 24 \cdot \frac{\sigma_3}{\sigma_1} \cdot \frac{(k_BT)^2}{q^2}. \quad (3)$$

This definition is based on a power-series expansion of Eq. (2) and is chosen such that in the regular hopping model, the hopping length a is given by

$$a = a_{app}. \quad (4)$$

Real solid electrolytes are often complex disordered materials (e.g. structurally disordered crystals, glasses, polymers, nanocomposites) with ions moving in a disordered potential landscape quite different to the regular hopping model. In this case, it is a theoretical challenge to elucidate the physical meaning of the apparent hopping distance a_{app} and to find out in what way it is related to pecularities in the potential landscape of the ions in the respective material.

In experiments, σ_1 and σ_3 can be obtained by applying different dc fields E to a thin sample and by fitting the detected current densities $j(E)$ to Eq. (1). Using this method, no information is available, however, about Joule heating effects. Joule heating may lead to an increase of the sample temperature, resulting in an increase of the ionic conductivity. Therefore, it is advantageous to use ac electric fields rather than dc fields. A nonlinear ionic conductivity leads to higher harmonic contributions to the current density spectrum, while this is not the case for Joule heating [3]. According to Eq. (1), the application of a sinusoidal electric field $E(t) = E_0 \cdot \sin(\omega t)$ leads to the following expression for the current density being

in phase with the electric field, j':

$$
\begin{aligned}
j' &= \sigma_1' \cdot E_0 \cdot \sin(\omega t) \\
&+ \sigma_3' \cdot (E_0)^3 \cdot \sin^3(\omega t) \\
&+ \sigma_5' \cdot (E_0)^5 \cdot \sin^5(\omega t) + \ldots \\
&= \sigma_1'(\omega) \cdot E_0 \cdot \sin(\omega t) \qquad (5) \\
&+ \frac{3}{4} \sigma_3'(\omega) \cdot (E_0)^3 \cdot \sin(\omega t) \\
&- \frac{1}{4} \sigma_3'(3\omega) \cdot (E_0)^3 \cdot \sin(3\omega t) \\
&+ \frac{10}{16} \sigma_5'(\omega) \cdot (E_0)^5 \cdot \sin(\omega t) \\
&- \frac{5}{16} \sigma_5'(3\omega) \cdot (E_0)^5 \cdot \sin(3\omega t) \\
&+ \frac{1}{16} \sigma_5'(5\omega) \cdot (E_0)^5 \cdot \sin(5\omega t) \\
&+ \ldots
\end{aligned}
$$

Thus, the higher harmonic currents can be used to determine values for the higher order–conductivity coefficients σ_3, σ_5 etc., while Joule heating effects can be definitely excluded as the reason for the field dependence of the current [3]

In Fig. 1 we show a schematic illustration of an experimental setup for nonlinear ac conductivity measurements on thin ion-conducting glass samples. The sample thickness is typically in the range from 60-100 μm, and we use ac voltages with amplitudes up to 500 V for achieving ac electric fields that are sufficiently high for detecting higher-harmonic currents. The thin glass samples are attached to a highly resistive quartz glass tube (conductivity $< 10^{-16}$ S/cm) by means of a high-voltage resistant Araldite glue (Vantico). The quartz tube with the attached sample is placed inside a quartz glass container. Both the quartz glass tube and the quartz glass container are filled with a liq-

uid electrolyte containing the same type of mobile cation as the glass sample. Platinum wires connected to the high-voltage measurement system are dipped into the liquid electrolyte. Since the electrical resistance of the liquid electrolyte is several orders of magnitude lower than the resistance of the glass samples, there is virtually no voltage drop in the liquid electrolyte, but the voltage applied to the platinum wires drops completely in the glass samples. Therefore, the liquid electrolyte solutions act as non-blocking electrodes.

The high-voltage measurement system is based on the Novocontrol Alpha–AK high resolution dielectric analyser, which is equipped with a broadband high-voltage amplifier, a broadband dielectric converter and a high-voltage sample head. A schematic illustration of the setup is shown in Fig. 2. The high-voltage system provides a frequency range from 3 μHz to 10 kHz, a maximum voltage of 500 V, and a current resolution of 5 fA. The digital waveforms of sample voltage and current are numerically Fourier transformed by a digital processor in the Alpha–AK analyser. Thereby, the amplitudes and phases of the base wave and of higher harmonics in the current spectrum are determined with respect to the sinusoidal voltage. Higher harmonics are detectable, if their amplitude is at least 10^{-3} of the base wave amplitude. The sample temperature is controled by the Novocontrol Quatro Cryosystem.

In Fig. 3 we show results for the base current density $j'(\nu)$ (closed symbols) and for the higher harmonic current density $j'(3\nu)$ (open sym-

bols), measured after applying a sinusoidal electric field with amplitude $E_0 = 58.8$ kV/cm to a Na^+ ion conducting glass with chemical composition $0.2\ Na_2O \cdot 0.8\ SiO_2$. Both $j'(\nu)$ and $j'(3\nu)$ are normalised by the field amplitude E_0 and are plotted versus frequency ν at two different temperatures, $T = 293$ K and 313 K. The $j'(\nu)/E_0$ curves reflect the frequency dependence of the low–field conductivity $\sigma_1'(\nu)$. The low-field conductivity exhibits the typical features known for solid electrolytes, i.e. dc conductivity plateau at low frequencies and dispersive conductivity at higher frequencies. The $j'(3\nu)/E_0$ curves exhibit a low-frequency plateau as well. According to Eq. (5), we can write the following expression for $j(3\nu)$:

$$
\begin{aligned}
\frac{-4 \cdot j'(3\nu)}{E_0} &= \sigma_3'(3\nu) \cdot (E_0)^2 \\
&+ \frac{5}{4} \sigma_5'(3\nu) \cdot (E_0)^4 \\
&+ \ldots \qquad (6)
\end{aligned}
$$

Thus, in a plot of $-4 \cdot j'(3\nu)/E_0$ versus $(E_0)^2$, the data should lie on a straight line with a slope of $\sigma_3'(3\nu)$, if the second term on the right-hand side of Eq. (6) is negligible. In Fig. 4 such a plot is shown for a temperature of $T = 293$ K and a frequency of $\nu = 0.0348$ Hz. This frequency is in the plateau regime of $j'(\nu)$ and $j'(3\nu)$. A closer look at Fig. 4 reveals that the data do *not exactly* lie on a straight line, but on a curve with a slightly negative curvature. Therefore, we fitted the data by a second–order polynomial. From the linear term in this polynomial, we obtain directly σ_3'. The negative curvature of the data implies that σ_5' is negative.
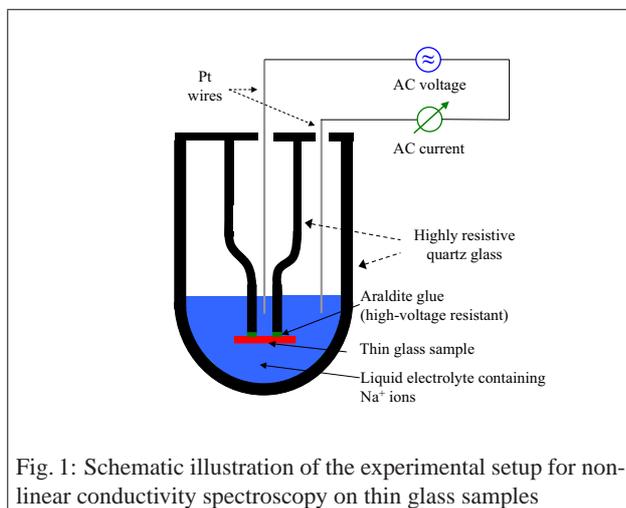
Fig. 1: Schematic illustration of the experimental setup for non-linear conductivity spectroscopy on thin glass samples
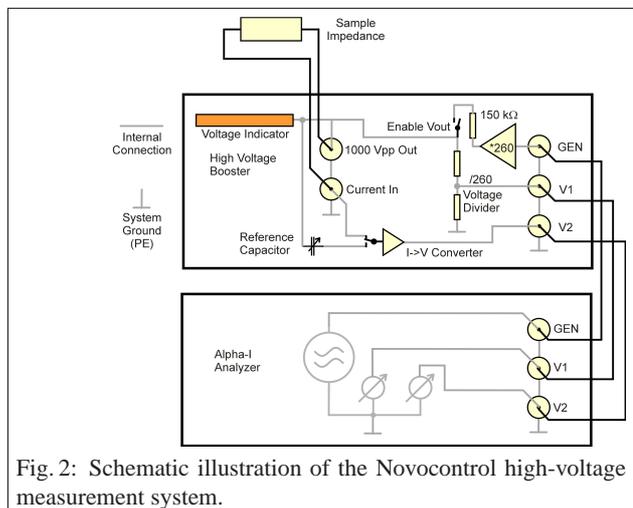
Fig. 2: Schematic illustration of the Novocontrol high-voltage measurement system.

However, the error in the curvature is so large that we can determine exclusively the sign of $\sigma_{5,dc}$, but not an accurate value.

Now, we can use the 'dc values' of σ_1 and σ_3 to calculate apparent jump distances a_{app} via Eq. (3). In Fig. 5, a_{app} is plotted versus temperature T for three different Na$^+$ ion conducting silicate glasses. The obtained values are in the range from about 40 Å to about 55 Å, i.e. the apparent jump distances are much larger than typical distances between nearest-neighbor sites (about 2.5-3 Å in molecular dynamics simulations [5]). For all three glasses, a_{app} decreases with increasing temperature.

In order to obtain a better understanding of the physical meaning of the absolute values of a_{app} and of its temperature dependence, theoretical analyses were carried out on one-dimensional single-particle disordered hopping models [4]. While the large apparent jump distances are reproduced in these hopping models, there are also clear discrepancies between the models and the experimental data [4]. The discussion of these discrepancies is, however, beyond the scope of this article and will be published in detail in a future paper [6]. Results for $j(E)$ in two- and three-dimensional models are not yet available. This will be the subject of future work.

References

[1] P. Vinatier, Y. Hamon, in *Charge Transport in Disordered Solids*, ed. S. Baranovski, Wiley 2006.

[2] N. F. Mott, E. A. Davis, *Electronic processes in Non-Crystalline Materials*, Clarendon, London, 1979.

[3] S. Murugavel, B. Roling, *J. Non-Cryst. Solids* **351** (2005) 2819.

[4] A. Heuer, S. Murugavel, B. Roling, *Phys. Rev. B* **72** (2005) 174304.

[5] A. Heuer, M. Kunow, M. Vogel, R. D. Banhatti, *Phys. Chem. Chem. Phys.* **4** (2002) 3185.

[6] B. Roling, S. Murugavel, A. Heuer, L. Luehning, R. Friedrich, S. Roethel, to be published.

Bernhard Roling* and Sevi Murugavel†
*Institute of Physical Chemistry, University of Marburg, Hans-Meerwein-Straße, 35032 Marburg, Germany.
†Department of Physics and Astrophysics, University of Delhi, Delhi 110 007, India.
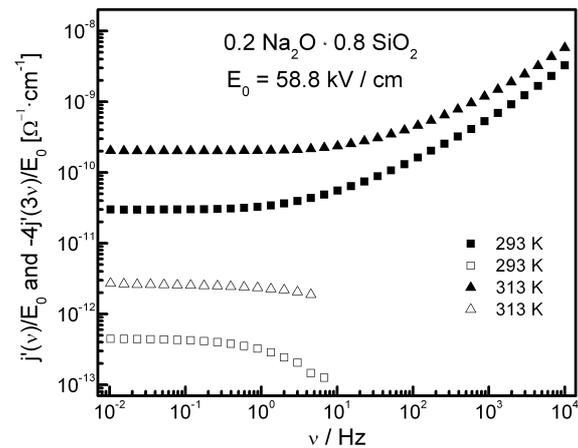
Fig. 3: Base current density $j'(\nu)$ (closed symbols) and higher harmonic current density $j'(3\nu)$ (open symbols), measured after applying a sinusoidal electric field with amplitude $E_0 = 58.8$ kV/cm to a 0.2 Na$_2$O · 0.8 SiO$_2$ glass sample.
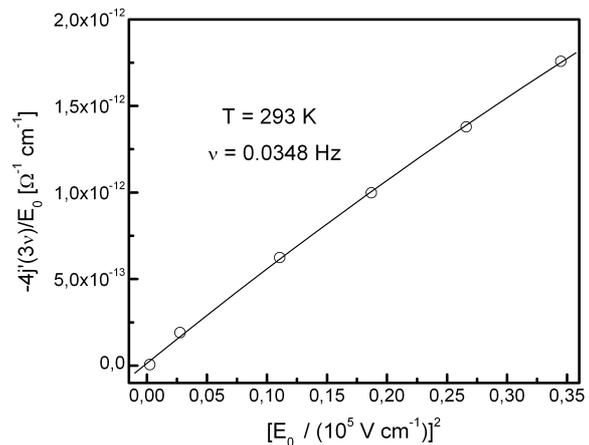
Fig. 4: Plot of $-4 \cdot j'(3\nu)/E_0$ versus $(E_0)^2$ for the 0.2 Na$_2$O · 0.8 SiO$_2$ glass at of $T = 293$ K and $\nu = 0.0348$ Hz. The solid line denotes a fit by a second-order polynomial.
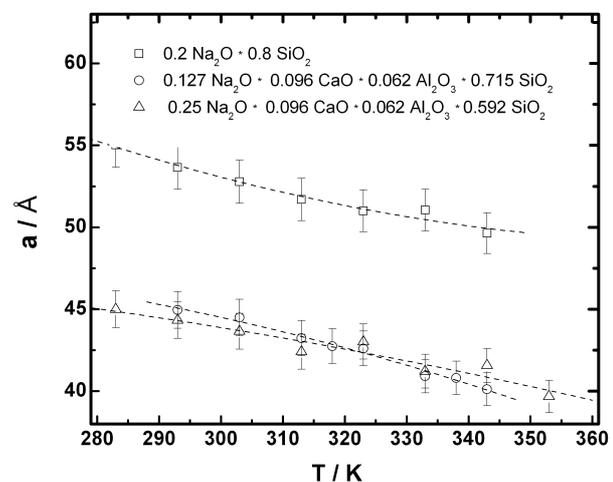
Fig. 5: Apparent jump distance a_{app} versus temperature T for three different Na$^+$ ion conducting glasses. The solid lines are drawn to guide the eye.

Meeting the Challenges of the 21st Century - Novel Applications of Broadband Dielectric Spectroscopy

Advanced Research Workshop

Suzdal, Russia, July 22 to 26, 2007

Broadband Dielectric Spectroscopy (BDS) is besides Nuclear Magnetic Resonance (NMR) and Infrared (IR) Spectroscopy the dominating experimental technique to study molecular dynamics and charge transport in soft and solid condensed matter. It is obvious that it has immediate impact on many modern technological challenges like, to name a few, liquid crystalline displays, ionic conductors in fuel cells and polymer (light weight) batteries, molecular dynamics in nanometric confinement, glassy dynamics and biological systems.

In the Advanced Research Workshop (ARW) sponsored by NATO with the Public Diplomacy Division, all these topics were addressed: Rotational and translational diffusion as measured by Broadband Dielectric Spectroscopy; Molecular dynamics in nanometric confinement; Dielectric spectroscopy in relation to other spectroscopic techniques; Broadband Dielectric Spectroscopy and charge transport phenomena; Dielectric spectroscopy in biological systems; Dielectric relaxation phenomena in polymers and glass forming liquids. Additionally panel discussions were arranged in which the following topics were addressed: Molecular dynamics at nanometric scales; Charge transport in ionic glassy systems; Dielectric properties of biological macromolecules and living biological matter. Furthermore two poster sessions were arranged where especially the younger scientists could present their latest results. Well-known scientists from Russia, Germany, France, USA, Israel, Belgium, Switzerland, Greece, Portugal, Japan, etc. participated in the conference. About 25 % of the participants were young scientists. The codirectors of the ARW, Profs. A. Khokhlov and F. Kremer, would like to thank - also in the name of the participants and the scientific community - NATO for the generous support.

F. Kremer, University of Leipzig

Announcement: Workshop "Broadband Dielectric Spectroscopy And Its Applications"

Responding to frequent demand from scientists interested in Broadband Dielectric Spectroscopy (BDS), Novocontrol Technologies announces its first workshop entitled "Broadband Dielectric Spectroscopy And Its Applications" to take place **July 24-25, 2008**, at the **University of Leipzig**, Germany under the guidance of Prof. F. Kremer.

The workshop will not only give an overview on the basics of this experimental technique, but also will elaborate on the following topics:

- fundamentals of Broadband Dielectric Spectroscopy (BDS)

- comparison to other spectroscopic techniques

- relaxational dynamics in glass forming liquids and polymers

- rotational and translational motion

- charge transport phenomena

Seminar blocks will be complemented by hands-on experience—under professional guidance, participants perform and evaluate their own experiments, if possible on their own samples.

The regular participation fee for this two-day workshop will be € 1500 (€ 700 for academic users). The number of participants is limited. Spaces are allocated on a first come - first serve basis.

Prospective participants are kindly asked to register by email to **workshop@novocontrol.de**.

D. Wilmer, Novocontrol

New Novocontrol High Voltage Extension HVB 4000

In the last couple of years, Novocontrol Technologies has constantly developed and extended its set of test interfaces for one of its key products, the broadband high-resolution gain-phase analyser Alpha-A. We currently offer three "'families'" of test interfaces, focussing on (i) dielectric spectroscopy (ii) electrochemical applications and, (iii) high-field/non-linear applications.

Responding to the increased demand for our high voltage test interfaces (HVB 300 and HVB 1000) and intending to lift the current limitation of $500\,V_p$, Novocontrol has developed its new HVB 4000 in order to extend the maximum voltage by a factor of four.

Our new combination of Alpha-A mainframe and HVB 4000 test interface delivers up to $\pm 2000\,V_p$ AC and/or DC bias voltage to the sample, covering the frequency range from $3\,\mu Hz$ to $10\,kHz$. The accessible measurement range covers both high and low impedances, i.e., up to $10^{15}\,\Omega$) and down to $100\,\Omega$, respectively. Due to the high output impedance of $750\,k\Omega$ (selected for safety reasons), output voltages will decrease if samples with impedance below 1 MΩ are connected.

The new HVB 4000 system is fully supported by the recent version of our WinDETA software. Alternatively, it maybe fully controlled by GPIB commands issued to the Alpha-A.

D. Wilmer, Novocontrol

A New Database of Publications on Dielectric and Impedance Spectroscopy

We frequently receive questions from our customers asking for typical publications that describe the most recent and/or most important developments in Broadband Dielectric Spectroscopy. At Novocontrol Technologies, we feel that is is not only important to solve your technical problems in this field, but also to know about the most important scientific trends.

We, therefore, kindly ask you to let us know about your scientific progress in Dielectric and Impedance Spectroscopy, especially if your experimental results have been obtained with Novocontrol measuring systems. Please send us your publications, most preferentially by email to novo@novocontrol.com in portable document format (PDF). We plan to create a database and a list of corresponding links to be presented on our web site.

D. Wilmer, Novocontrol

OVERVIEW

BROADBAND DIELECTRIC AND IMPEDANCE SPECTROSCOPY
covering 16 frequency decades by Novocontrol Technologies
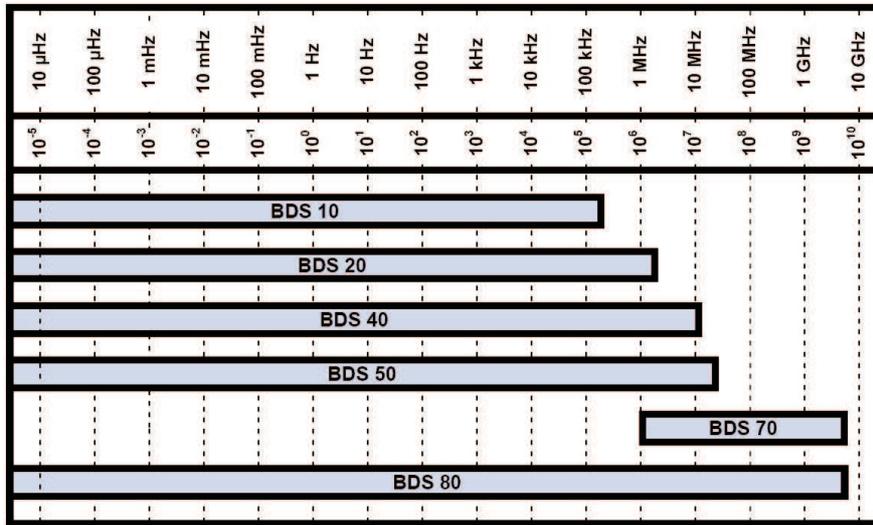
Factory and Head Office

Novocontrol Technologies GmbH & Co. KG

Germany
Obererbacher Straße 9
56414 Hundsangen/GERMANY
Phone: +49 6435 9623-0
Fax: +49 6435 9623-33
Mail: novo@novocontrol.de
Web: www.novocontrol.de
Contact: Dr. Dirk Wilmer

United Kingdom
Additional Technical and Sales Support for UK Customers
Headways, Shoulton, Hallow
Worcester, WR2 6PX, UK
Phone: +44 870 085 0744
Fax: +44 870 085 0745
Mobile: +44 7974 926 166
Mail: jed@novocontrol.de
Web: www.novocontrol.de
Contact: Mr Jed Marson

Agents

USA/Canada
Novocontrol America Inc.
8537 Purnell Ridge Road
Wake Forest, NC 27587 / USA
Toll free: +1 866 554 9904
Phone: +1 919 554 9904
Fax: +1 919 556 9992
Mail: novocontrolusa@earthlink.net
Contact: Mr. Joachim Vinson, PhD

Japan
Morimura Bros. Inc.
2nd Chemical Division
Morimura Bldg. 3-1, Toranomon 1-chome
Minato-Ku, Tokyo 105 / Japan
Phone: +81 3-3502-6440
Fax: +81 3-3502-6437
Mail: s-hasegawa@morimura.co.jp
Contact: Mr. Shintaro Hasegawa

People's Republic of China
GermanTech Co. Ltd
Room 706, No. 7 Building; Hua Qing Jia Yuan
Wu Dao Kou, Haidian District
Beijing, 100083 / China
Phone: +86 10 82867920/21/22
Fax: +86 10 82867919
Mail: contact@germantech.com.cn
Contact: Mrs. Xiaoyu Sun

Taiwan
JIEHAN Technology Corporation
No. 58, Chung Tai East Road, 404
Taichung / Taiwan
Phone: 886-4-2208-2450
Fax: 886-4-2208-0010
Mail: jiehantw@ms76.hinet.net
Contact: Mr. Peter Chen

South Korea
PST Polymer Science Technologies
Rm. 716, Hojung Tower, 528-13
Anyang-shi, Kyungki-Do, Korea
Phone: 031-507-8552
Fax: 031-448-6189
Mail: sunpoint@hanafos.com
Contact: Mr. Young Hong

Greece
Vector Technologies Ltd.
40 Diogenous Str.
15234 Halandri, Athens
Phone: +30 210 6858 008
Fax: +30 210 6858 118
Mail: info@vectortechnologies.gr
Contact: Mr. Vouvounas

Editor: Dirk Wilmer. Abstracts and papers are always welcome. Please send your manuscript to the editor.